Bond length compressibility in hard ReB_2 investigated by x-ray absorption under high pressure

2010 J. Phys.: Condens. Matter 22 045701

(http://iopscience.iop.org/0953-8984/22/4/045701)

J. Phys.: Condens. Matter **22** (2010) 045701 (7pp) doi:10.1088/0953-8984/22/4/045701

Bond length compressibility in hard ReB_2 investigated by x-ray absorption under high pressure

J Pellicer-Porres[1], A Segura[1], A Muñoz[2], A Polian[3] and A Congeduti[4]

[1] MALTA Consolider Team, ICMUV, Universidad de Valencia, c/Dr Moliner 50, 46100 Burjassot, Valencia, Spain
[2] MALTA Consolider Team, Departamento de Física Fundamental II, Universidad de la Laguna, 38204 La Laguna (Tenerife), Spain
[3] Physique des Milieux Condensés, CNRS-UMR 7602, Université Pierre et Marie Curie, B77, 4, place Jussieu, 75252 Paris Cedex 05, France
[4] Synchrotron SOLEIL, L'Orme des Merisiers, Saint-Aubin—BP 48, 91192 Gif-sur-Yvette Cedex, France

E-mail: Julio.Pellicer@uv.es

Received 9 September 2009, in final form 12 November 2009
Published 12 January 2010
Online at stacks.iop.org/JPhysCM/22/045701

Abstract
This work describes x-ray absorption measurements under high pressure in ReB_2, complemented by *ab initio* calculations. The EXAFS analysis yields the average Re–B bond compressibility, which turns out to be $\chi_{ReB} = 5.6(9) \times 10^{-4}$ GPa^{-1}. Combining this information with previous x-ray diffraction experiments we have characterized the network of covalent bonds responsible for the rigidity of the structure. The main conclusion is that the compression is anisotropic and nonhomogeneous, reflecting bonding differences between Re–B and B–B bonds and also between nonequivalent Re–B bonds. The layer defined by boron atoms tends to become flatter under high pressure. As a consequence, the structural rigidity, necessary to attain high hardness values, is compromised.

(Some figures in this article are in colour only in the electronic version)

1. Introduction

The quest for superhard materials has recently focused attention on ReB_2. Following recent results [1], this compound combines the properties of high hardness, low compressibility and resistance to high differential stress. Moreover, its synthesis does not necessitate high pressure conditions, as do other ultrahard materials like cubic BN, BC_2N or B_6O. However, according to [2] and [3], the reported hardness [1], 48 GPa under an applied load of 0.49 N, does not constitute a definitive argument to consider ReB_2 as a superhard material. Measurements at higher loads, reaching the asymptotic regime, where there is no load dependence, yield hardness values [1, 4, 5] near 30 GPa. In any case ReB_2 is claimed to be the hardest metallic compound [5].

Hardness is deduced from the size of the indentation mark left on the material by the tip of an indenter. The size of the indentation depends [6] on the material's response to the compression stress, its capacity to withstand deformations in a direction different from the applied load and its resistance to plastic flow. High hardness thus requires high bulk modulus B, shear modulus G and shear strength. In ReB_2, according to experiments [1, 7], B = 320–360 GPa and G = 280 GPa. The shear strength has been calculated in [8], resulting in 34 GPa for the $(001)\langle 100\rangle$ slip system. The hardness and elastic properties of ReB_2 have been linked [1, 8, 9] to the combination of a high electron density together with the formation of a network of strong, covalent bonds. The electronic distribution and bond population have been extensively studied in the literature [8–11].

High pressure is a versatile tool that can be used to characterize the effect of altering the electron density and to explore the changes induced in covalent bonding. This idea was present in the original work of Chung *et al* [1], where

the compressibility of the lattice parameters and bulk modulus of the material was measured by x-ray diffraction (XRD) experiments under high pressure. However, no information about the behavior of the covalent bonds under high pressure was given.

XRD under high pressure has experimental limitations (like, for example, diamond absorption, preferential orientation or low statistics) which make the extraction of information from the intensity of diffraction reflections not always straightforward. This is particularly the case in ReB_2, due to the large atomic number difference between Re and B. As a consequence, the effect of pressure on the position of boron inside the unit cell is not known. On the contrary, x-ray absorption (XAS) is a local technique which directly probes the local environment of the absorbing atom. In this work we have performed XAS measurements under high pressure at the Re-L_3 edge, which give direct access to the Re–B bond length. The high symmetry of the unit cell then allows a full characterization of the network of covalent bonds.

This work is organized as follows. In section 2 the experimental procedures and calculation scheme are presented. In section 3.1 the calculated results for the lattice parameters are discussed. Section 3.2 is devoted to the extended x-ray absorption fine structure (EXAFS) analysis. The information yielded by EXAFS is used in section 4 to characterize the network of covalent bonds and analyze the structural rigidity. We conclude in section 5.

2. Experiment and calculation

2.1. Experiment

ReB_2 was prepared by mixing powdered B (99.9%, LTS (Chemical) Inc.) and Re (99.995%, Aldrich) with a molar ratio of 2.5:1. A pellet was formed with an oil press. It was introduced in an alumina crucible, which was heated up to 1300 K during 4 h in vacuum conditions (5×10^{-5} mbar). The ReB_2 structure was checked by x-ray diffraction. A single peak related to an unidentified impurity phase was also observed. Its integrated intensity corresponds to 5% of the most intense ReB_2 reflection, the (101), or 1% of the whole integrated intensity. We conclude that the impurity is present in small proportion, not exceeding 5%.

XAS experiments were performed at the ODE beamline in the Soleil Synchrotron (St Aubin, Paris, France). ODE operates in the dispersive mode. A bent silicon crystal is used to select the energy range of interest, containing the absorption edge under study (Re L_3, 10.535 keV). The bent crystal also focuses the beam horizontally and defines a spot of 50 μm (a mirror focuses the beam down to 40 μm in the vertical direction). The whole spectrum was measured in one shot using a position sensitive detector. The energy scale was calibrated by measuring the spectra of $ReNaO_4$ and metallic Ir and comparing them with the same spectra measured with a scanning XAS spectrometer. High pressures were generated using a membrane diamond anvil cell (MDAC) [12]. The diamond anvils are single crystals which unavoidably diffract both the incident and transmitted beams, introducing glitches in the spectrum. The MDAC must then be oriented in order to move the glitches out of the region of interest. This procedure is considerably facilitated in the dispersive configuration, where the shifts of the glitches associated with changes in the MDAC orientation are observed in real time. The reference spectrum (I_0) used to calculate the absorption was measured outside the MDAC.

Dispersive XAS measurements in third generation synchrotrons are extremely demanding in terms of sample homogeneity. The MDAC loading procedure was designed in order to get as homogeneous a sample as possible. In a first step we formed a 7 μm pellet (total absorption $\mu x \approx 1.7$, edge jump $\Delta\mu x \approx 1$), compressing the ReB_2 powder between the two diamonds. In a second step we laid the pellet on the diamond surface, inside the 250 μm gasket hole. The remaining free space was filled with the pressure transmitting medium, NaCl. Finally, we added a small ruby chip as a pressure sensor [13, 14]. The ruby doublet broadening indicated no significant loss of hydrostatic conditions up to 20 GPa. The experiment was performed on two successive loadings, giving very reproducible results, as can be seen below.

2.2. Calculation details

Total-energy calculations were done within the framework of the density-functional theory (DFT) [15, 16] and the pseudo-potential method using the Vienna *ab initio* simulation package (VASP), a detailed account of which can be found in [17]. The exchange and correlation energy was taken in the generalized gradient approximation (GGA) according to the Perdew–Burke–Ernzerhof (PBE) prescription [18]. The projector augmented wave (PAW) scheme [19, 20] was adopted and the semicore 5p electrons of Re were dealt with explicitly in the calculations. The set of plane waves used extended up to a kinetic-energy cut-off of 910 eV. This large cut-off was required to deal with the B atoms within the PAW scheme to ensure highly converged results. The Monkhorst–Pack grid used for Brillouin-zone integrations ensured highly converged results (to about 1 meV/f.u.). At each selected volume, the structures were fully relaxed to their equilibrium configuration through the calculation of the forces on atoms and the stress tensor. In the relaxed equilibrium configuration, the forces are less than 0.002 eV $Å^{-1}$ and the deviation of the stress tensor from a diagonal hydrostatic form is less than 0.1 GPa.

3. Results

3.1. Lattice parameters

The ReB_2 structure (figure 1) is described with a hexagonal unit cell (space group $P6_3/mmc$). The measured lattice parameters at ambient pressure are $a = 2.899$ Å and $c = 7.473$ Å, to be compared with previous data from [21]: $a = 2.9$ Å and $c = 7.478$ Å. Both angular dispersive [1] and energy dispersive [22] XRD experiments under high pressure are available in the literature. The measured lattice parameters are represented in figure 2. The unit cell compression is anisotropic, with the c-axis decreasing more slowly than the

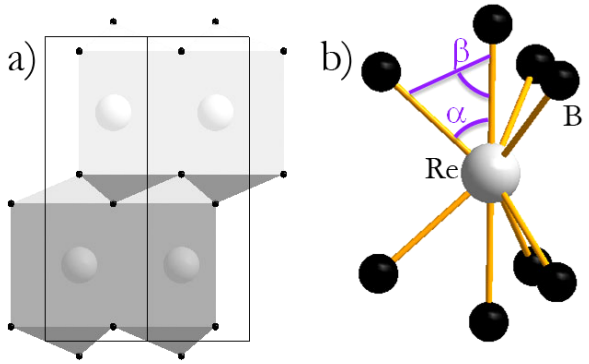

Figure 1. (a) Two adjacent ReB_2 unit cells viewed from the [010] direction. (b) Perspective view of the Re first coordination shell with characteristic bonding angles.

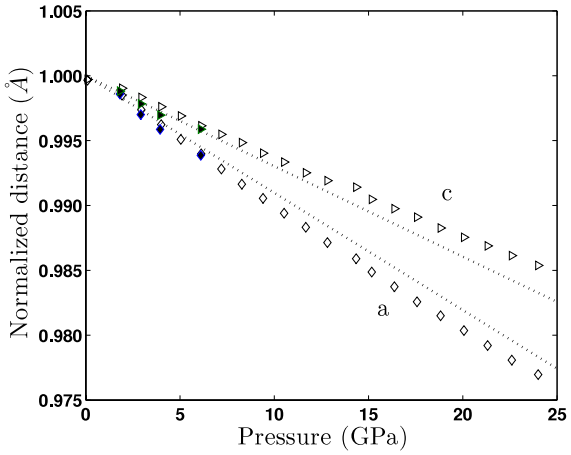

Figure 2. Relative lattice parameters as a function of pressure. Dotted lines and filled symbols represent angular dispersive [1] and energy dispersive [22] XRD data, respectively. Hollow symbols correspond to the *ab initio* calculations obtained in this work.

a-axis. XRD results agree within the experimental error. However, energy dispersive XRD has been performed up to 6 GPa only. Given the pressure range studied in the present work (up to 25 GPa) and the uncertainties introduced in the extrapolation procedure by the significant data dispersion, we will only consider in the following the results of angular dispersive XRD. The bulk modulus measured by angular dispersive XRD is $B = 360$ GPa (with B' fixed to 4). The compressibility associated with each cell axis is $\chi_a = -\frac{1}{a}\frac{\partial a}{\partial P} = 9 \times 10^{-4}$ GPa^{-1} and $\chi_c = 7.0 \times 10^{-4}$ GPa^{-1}.

We now make a comparison with the results of the *ab initio* calculations. The computed ambient pressure cell dimensions are $a = 2.911$ Å and $c = 7.520$ Å. Their evolution under high pressure is presented in figure 2 as hollow symbols. Their compressibilities are $\chi_a = 1.0 \times 10^{-3}$ GPa^{-1} and $\chi_c = 6.2 \times 10^{-4}$ GPa^{-1}. The calculations result in a difference in compressibility of the two axes larger than that found experimentally. Other calculations available in the literature [11, 23] show similar results. The bulk modulus (B) and its pressure derivative have been extracted from a Murnaghan fit to the calculated equation of state, yielding

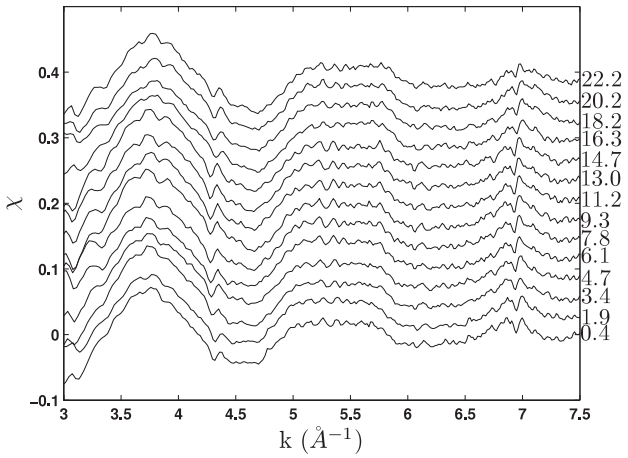

Figure 3. ReB_2 XAS signal as deduced from measurements at the Re L_3 edge under high pressure. Labels next to each spectrum indicate pressure in GPa.

$V_0 = 55.23(3)$ Å^3, $B = 350(15)$ GPa and $B' = 2.9(1.2)$. If the fit of the *ab initio* equation of state is performed with the B' value constrained to 4, we obtain $B = 337(5)$ GPa.

3.2. EXAFS analysis

The absorption edge energy was set experimentally at the zero of the second derivative of the absorption spectra. The EXAFS signal (figure 3) was extracted from the normalized spectra using a single cubic spline determined by least squares approximation. The high k limit of the spectra is limited by distortions induced by energetic inhomogeneities of the focus point, which imposed exceptional sample homogeneity, as described in section 2. In the selected wavelength range the EXAFS signal is stable and shows a progressive shift to higher k values associated with bond length contraction.

The rhenium coordination sphere in ReB_2 is constituted (figure 1(b)) by eight boron atoms in a 2+6 configuration, with close distances: $d_{ReB_1} = 2.23$ Å and $d_{ReB_2} = 2.25$ Å. The short distance corresponds to two boron atoms in axial configuration along the hexagonal c-axis. The other six boron atoms are disposed in a triangular prismatic configuration. The second shell comprises the six rhenium neighbors characteristic of a hexagonal layer, situated at 2.9 Å.

The limited k range imposed restrictions on the EXAFS analysis. We show in figure 4 the Fourier transform of the EXAFS signal comprised between 3.2 and 7.5 Å^{-1}, calculated using a Hanning apodization window. It is clear that the first pair of Re–B distances cannot be resolved. Moreover, the Fourier transform peak extending from 0.8 to 3.0 Å includes both the Re–B shell and the second neighbor Re–Re contribution. The structural model used to fit the EXAFS signal included these two shells, the first one representing an average Re–B distance and the second one standing for the Re–Re contribution. We used the FEFF8.2 code [24] to calculate the phases and amplitudes corresponding to both shells. We performed a self-consistent calculation with a cluster of 87 atoms extending 5.5 Å from the absorbing

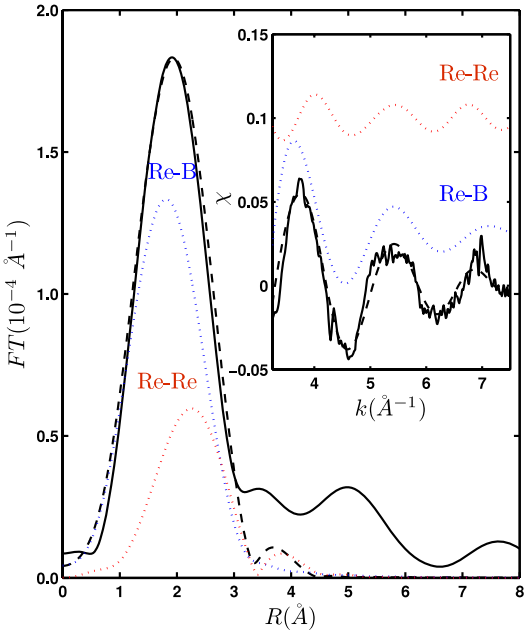

Figure 4. Pseudo-pair distribution function (main figure) and EXAFS signal (inset) at 4.7 GPa. The experimental data are drawn with a continuous line. The EXAFS fit is represented by a dashed line. The contributions of the two individual shells considered in the model are indicated with dotted lines.

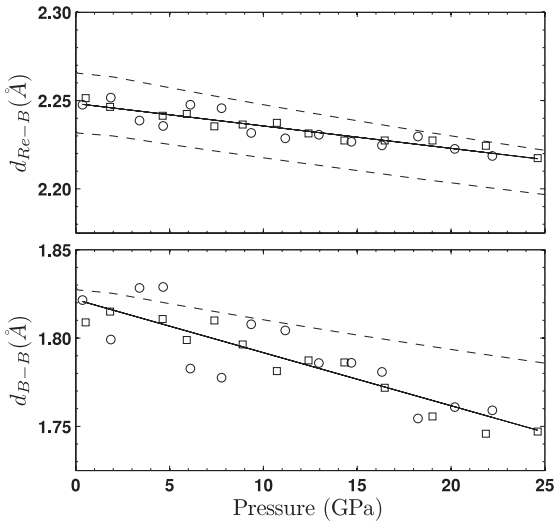

Figure 5. Bond length compression under high pressure. Symbols represent results from the EXAFS analysis corresponding to two different samples. However, whereas the Re–B distances displayed in the upper panel are obtained directly from the EXAFS analysis, the B–B distances represented in the lower panel have been calculated combining EXAFS and XRD data (see text). Continuous lines are the result of linear fits. Dashed lines represent the results of *ab initio* calculations.

atom. The Hedin–Lundqvist self-energy was used to model the energy dependent exchange correlation potential. The EXAFS fits were performed in k space. The fit parametrized many-body relaxation effects through the amplitude reduction factor S_0^2. The difference between the theoretical and experimental energy scale is taken into account introducing an energy shift E_0. Both the amplitude reduction factor and the energy shift were deduced from the ambient pressure spectrum, and then subsequently used in the high pressure fits of the two samples studied ($S_0^2 = 0.92$, $E_0 = 9.4$ eV). In order to further reduce the number of free parameters in the fit, the Re–Re distance at a given pressure was fixed at the value measured by XRD [1]. In this way there were only three parameters in each fit: the average Re–B distance, $d_{\mathrm{Re-B}}$, and the pseudo-Debye–Waller factors associated with the two shells, $\sigma^2_{\mathrm{Re-B}}$ and $\sigma^2_{\mathrm{Re-Re}}$. As an example, we show as a dotted line in figure 4 the fit corresponding to the spectrum taken at 4.7 GPa, as well as the contribution from the two shells. The parameters obtained in the fit are compiled in table 1. Care must be taken in order to interpret the amplitude values of each shell. The main reason for the relatively low value of the Re–Re amplitude is not associated with the pseudo-Debye–Waller factor (at least at low pressures, see below) but with the markedly different wavelength dependence of the backscattering amplitudes of boron and rhenium atoms. Light boron atoms have backscattering amplitudes peaking at 1.8 $\AA^{-1}$. Heavy Re atoms show a backscattering amplitude with a small contribution at low k values which grows (nonmonotonically) up to 15 $\AA^{-1}$. As a consequence, the k range employed in the EXAFS analysis reinforces the boron contribution.

Table 1. Parameters employed in the fit to the EXAFS signal measured at 4.7 GPa (represented in figure 4). The energy shift ($E_0 = 9.4$ eV) and amplitude reduction factor ($S_0^2 = 0.92$) were deduced from the ambient pressure spectrum, and then subsequently used in the high pressure fits of the two samples studied. At a given pressure, we introduce in the fit the Re–Re distance measured by x-ray diffraction [1].

Shell	Coordination number	Distance (Å)	Pseudo-Debye–Waller (Å^2)
Re–B	8	2.24(2)	0.007(2)
Re–Re	6	2.89	0.007(2)

The evolution of $d_{\mathrm{Re-B}}$ under high pressure obtained from the two independent experiments is plotted as symbols in figure 5. A linear fit yields $d_{\mathrm{Re-B}} = 2.248(3) - 1.3(2) \times 10^{-3} P$, where $d_{\mathrm{Re-B}}$ is in Å and P in GPa. Equivalently, the compressibility is $\chi_{\mathrm{ReB}} = -1/\mathrm{d}\partial\, \mathrm{d}/\partial P = 5.6(9) \times 10^{-4}$ GPa^{-1}. This result will be discussed in section 4.

The pseudo-Debye–Waller factor (DW) associated with the Re–B length is approximately constant, $\sigma^2_{\mathrm{Re-B}} = 0.005(1) - 2(5) \times 10^{-5} P$, where σ^2 is in Å^2. The ambient pressure value is self-consistent with the structural model employed in the EXAFS analysis. Representing the two Re–B distances, 2.223 Å and 2.255 Å, with a single shell is equivalent to introducing a static disorder of the order of $\sigma^2 = 0.0007$ Å^2, which is only a small fraction of the DW measured. With respect to the pressure dependence, the harmonic contribution to the DW should decrease when pressure is increased as a consequence of the bond length contraction. A small decrease is in fact observed in the data. However, given the data dispersion, we do not consider the decrease significant and conclude that the static disorder is slightly increasing in the

B shell. The DW associated with the second shell clearly increases, $\sigma^2_{\mathrm{Re-Re}} = 0.006(1) + 1.4(8) \times 10^{-4} P$, so does the static disorder associated with the Re–Re distance.

4. Discussion

4.1. Effect of high pressure on the bond network

As pointed out in section 1, the existence of a network of directional, covalent bonds is the key to the remarkable mechanical properties of ReB_2 (together with the high electron density). We have just described the compressibility of the Re–B bond. We now focus on the pressure dependence of the B–B bond.

The ReB_2 structure (figure 1) is highly symmetrical. Rhenium atoms occupy hcp sites. The only internal parameter, u, locates B atoms along the c-axis and determines the Re–B bond length. Combining the Re–B distance obtained in the EXAFS analysis and previous high pressure XRD determinations of the lattice parameters, it is then possible to calculate u. However, one must take into account that the EXAFS Re–B distance corresponds to two kinds of boron backscatterers situated at distances given by

$$\begin{aligned} d_{\mathrm{ReB}_1} &= (u - 0.25)c \\ d_{\mathrm{ReB}_2} &= \sqrt{\frac{a^2}{3} + (0.75 - u)^2 c^2}. \end{aligned} \tag{1}$$

We assume that the Re–B distance obtained in the EXAFS analysis corresponds to the average distance, i.e.

$$d^{\mathrm{EXAFS}} \equiv \bar{d}_{\mathrm{ReB}} = \frac{2d_{\mathrm{ReB}_1}(u) + 6d_{\mathrm{ReB}_2}(u)}{8}. \tag{2}$$

The internal parameter u is obtained by numerically solving this last equation. The lattice parameters employed correspond to those measured by angular dispersive XRD [1]. Results from the two experiments performed are presented in figure 6 with symbols. The continuous line represents a linear fit. u decreases very slowly, only 1% in the whole 25 GPa range explored. In their turn, *ab initio* calculations yield a constant internal parameter. The difference between the *ab initio* calculations and the experiment is very small (again of the order of 1% at the highest pressures attained). It could be argued that the observed mismatch is associated with the slight disagreement between the calculated and measured [1] compressibility of the lattice parameters. In order to clarify this point, we have checked that the internal parameter resulting from *ab initio* a and c lattice parameters and experimental d_{EXAFS} shows a similar pressure behavior to the one obtained using only measured parameters.

Finally, the B–B distance is given by

$$d_{\mathrm{BB}} = \sqrt{\frac{a^2}{3} + (1 - 2u)^2 c^2}. \tag{3}$$

The evolution of the B–B distance under high pressure is presented in figure 5. The measured compressibility is $\chi_{\mathrm{BB}} = 1.6(3) \times 10^{-3}$ GPa^{-1}, the calculated one is $\chi_{\mathrm{BB}} = 0.9(1) \times 10^{-3}$ GPa^{-1}. The magnitude of the B–B bond length

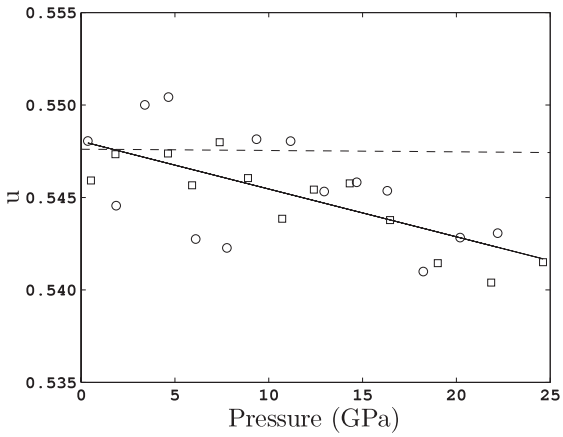

Figure 6. Pressure behavior of the internal parameter in ReB_2. Symbols are deduced from calculations involving both the EXAFS determined Re–B bond length and XRD data (see text). Squares and circles correspond to EXAFS data obtained from two different samples. The fit to the experimental data and the results obtained by *ab initio* calculations are represented by a continuous and a dashed line, respectively.

reduction in ReB_2 can be compared with that measured in MgB_2. In MgB_2, boron atoms form *flat* covalently bonded hexagonal layers. Mg atoms are also arranged in hexagonal layers interleaved between the boron ones. Each boron atom is surrounded by three other boron atoms at $\frac{\sqrt{3}}{3}a$. In this material it is possible to calculate the compressibility of the B–B bond from the pressure dependence of the a axis, measured [25] by XRD. The result is $\chi_{\mathrm{BB}} = 1.8(2) \times 10^{-3}$ GPa^{-1}, which is very close to the experimental value obtained in ReB_2.

4.2. Structural rigidity

In order to present high hardness, a given material must have, among other requisites, a rigid structural topology [6]. The XAS measurements and, to a lesser extent, the *ab initio* calculations, show that the B–B bond compressibility is larger than the Re–B one. The geometrical consequences of this fact can be understood as follows. We recall that rhenium atoms are surrounded by boron atoms in a $2 + 6$ configuration. The six boron atoms at 2.25 Å define a triangular prism (figure 1). The prisms are arranged following the $ABAB\cdots$ stacking pattern characteristic of the hcp structure. The two boron atoms situated along the c-axis may be regarded as belonging to neighboring prisms from lower and upper stacking planes. From this point of view, the covalent B–B bonds would form a net joining neighboring prisms. The differences in compressibility between Re–B and B–B bonds show that the triangular prisms are harder to compress than the space between the prisms. This behavior can be related to the electronic distribution. The bonding properties in transition metal diborides have been discussed in [9] by means of the electronic localization function, showing that the Re–B bonds formed along the c-axis are clearly weaker than the Re–B bonds defining the prisms.

The analysis of the rigidity of the covalent bond network can be complemented with a study of angular variations

induced by high pressure. We consider the B–Re–B angle labeled α in figure 1(b) characteristic of the triangular prism. The Re–B–B angle, labeled β, is representative of the boron network joining the prisms. The α angle remains approximately constant under high pressure. The prisms then behave as nearly rigid units which remain practically undistorted under applied pressure. However, following the experimental results, the β angle increases from 67.0 to 69(1), revealing a tendency of the boron layers to become flatter at high pressure. The variation of the β angle is not reproduced in the calculations. The discrepancy can be attributed to the slight disagreement between the *ab initio* and experimental values of the internal parameter as well as to the effect of accumulated errors in the calculation of the experimental angle.

With the aim of judging the magnitude of the angular distortions found, we compare our results with those obtained in other compounds. In ultrahard materials like diamond or cubic BN the bonding angles are not modified by high pressure. Another relevant material, metallic Re, displays a hexagonal closed packed structure which could in principle be distorted by high pressure. However, this is not the case, as it has been shown [26] that the c/a ratio remains constant under pressure. We have to resort to other types of materials in order to establish comparisons. In the InSe layered semiconductor, where the intralayer bonds are covalent and the interlayer interaction is close to being of the van der Waals type, the angle between the Se layers and the In–Se bond increases [27] nearly an order of magnitude faster than β in ReB_2 (in relative values). The angular change is associated with the increasing role of the interlayer interaction under high pressure. On the other hand, the variation observed in β is comparable to that observed in the polar semiconductor $CuGaO_2$ [28, 29]. The structure in this compound is defined by GaO_6 edge sharing octahedral layers. The GaO_6 layers are joined by O–Cu–O linear bonds perpendicular to the layers. The initially distorted octahedra tend to become more regular under high pressure.

We conclude that in ReB_2 the structural rigidity is compromised by a nonhomogeneous charge distribution, which is altered by high pressure and evidenced by the different compressibility of Re–B and B–B bonds as well as by the slight angular distortion measured.

5. Conclusions

X-ray absorption measurements at the Re L_3-edge have been used to characterize the compressibility and angular distortions of the covalent bond network in ReB_2. The experimental study is complemented by *ab initio* calculations. The main conclusion is that the compression is anisotropic and nonhomogeneous, reflecting bonding differences between Re–B and B–B bonds and also between nonequivalent Re–B bonds. The spaces around Re atoms defined by six boron atoms define triangular prisms which behave as nearly rigid units and which are harder to compress than the boron chains joining the prisms. As a consequence, the structural rigidity, necessary to attain high hardness values, is compromised.

Acknowledgments

We acknowledge the Ministerio de Ciencia y Tecnología of Spain (projects MAT2007-65990-C03-01, MAT2007-65990-C03-03 and MALTA Consolider Initiative, CSD2007-00045). We thank the SOLEIL synchrotron for granting us beamtime and especially the ODE staff for assistance during the experiment. AM acknowledges the facilities at the MareNostrum supercomputer.

References

[1] Chung H-Y, Weinberger M B, Levine J B, Cumberland R W, Kavner A, Yang J-M, Tolbert S H and Kaner R B 2007 Synthesis of ultra-incompressible superhard rhenium diboride at ambient pressure *Science* **316** 436–9

[2] Dubrovinskaia N, Dubrovinski L and Solozhenko V L 2007 Comment on 'Synthesis of ultra-incompressible superhard rhenium diboride at ambient pressure' *Science* **318** 1550c

[3] Qin J, He D, Wang J, Fang L, Lei L, Li Y, Hu J, Kou Z and Bi Y 2008 Is rhenum diboride a superhard material? *Adv. Mater.* **20** 4780–3

[4] Otani S, Korsukova M M and Aizawa T 2009 High-temperature hardness of ReB_2 single crystals *J. Alloys Compounds* **477** L28–9

[5] Levine J B, Nguyen S L, Rasool H I, Wright J A, Brown S E and Kaner R B 2008 Preparation and properties of metallic, superhard rhenium diboride crystals *J. Am. Chem. Soc.* **130** 16953–8

[6] Haines J, Léger J M and Bocquillon G 2001 Synthesis and design of superhard materials *Annu. Rev. Mater. Res.* **31** 1–23

[7] Koehler M R, Keppens V, Sales B C, Jin R and Mandrus D 2009 Elastic moduli of superhard rhenium diboride *J. Phys. D: Appl. Phys.* **42** 095414

[8] Zhang R F, Veprek S and Argon A S 2007 Mechanical and electronic properties of hard rhenium diboride of low elastic compressibility studied by first-principles calculation *Appl. Phys. Lett.* **91** 201914

[9] Chen X, Fu C L, Krčmar M and Painter G S 2008 Electronic and structural origin of ultraimcompressibility of 5d transition-metal diborides MB_2 (M = W, Re, Os) *Phys. Rev. Lett.* **100** 196403

[10] Zhou W, Wu H and Yildirim T 2007 Electronic, dynamical, and thermal properties of ultra-incompressible superhard rhenium diboride: a combined first-principles and neutron scattering study *Phys. Rev.* B **76** 184113

[11] Liang Y and Zhang B 2007 Mechanical and electronic properties of superhard ReB_2 *Phys. Rev.* B **76** 132101

[12] LeToullec R, Pinceaux J P and Loubeyre P 1988 The membrane diamond anvil cell: a new device for generating continuous pressure and temperature variations *High Pressure Res.* **1** 77

[13] Chervin J C, Canny B and Mancinelli M 2001 Ruby-spheres as pressure gauge for optically transparent high pressure cells *High Pressure Res.* **21** 305–14

[14] Mao H, Xu J and Bell P 1986 Calibration of the ruby pressure gauge to 800 kbar under quasi-hydrostatic conditions *J. Geophys. Res.* **91** 4673–6

[15] Hohenberg P and Kohn W 1964 Inhomogeneous electron gas *Phys. Rev.* **136** B864–71

[16] Kohn W and Sham L J 1965 Self-consistent equations including exchange and correlation effects *Phys. Rev.* **140** A1133–8

[17] Kresse G *Computer Code VASP* http://cms.mpi.univie.ac.at/vasp

[18] Burke K, Perdew J P and Ernzerhof M 1996 Generalized gradient approximation made simple *Phys. Rev. Lett.* **77** 3865

[19] Blöchl P E 1994 Projector augmented-wave method *Phys. Rev.* B **50** 17953–79
[20] Kresse G and Joubert D 1999 From ultrasoft pseudopotentials to the projector augmented-wave method *Phys. Rev.* B **59** 1758–75
[21] La Placa S J and Post B 1962 The crystal structure of rhenium diboride *Acta Crystallogr.* **15** 97–9
[22] Wang Y, Zhang J, Daemen L L, Lin Z, Zhao Y and Wang L 2008 Thermal equation of state of rhenium diboride by high pressure–temperature synchrotron x-ray studies *Phys. Rev.* B **78** 224106
[23] Zhu X, Li D and Cheng X 2008 Elasticity properties of the low compressible material ReB_2 *Solid State Commun.* **147** 301–4
[24] Rehr J J, Ankudinov A L, Ravel B and Conradson S D 1998 Real space multiple scattering calculation of XANES *Phys. Rev.* B **58** 7565
[25] Vogt T, Schneider G, Hriljac J A, Yang G and Abell J S 2001 Compressibility and electronic structure of MgB_2 up to 8 GPa *Phys. Rev.* B **63** 220505
[26] Vohra Y K, Duclos S J and Ruoff A L 1987 High-pressure x-ray diffraction studies on rhenium up to 216 GPa (2.16 mbar) *Phys. Rev.* B **36** 9790–2
[27] Pellicer-Porres J, Segura A, Muñoz V and San Miguel A 1999 High-pressure x-ray absorption study of InSe *Phys. Rev.* B **60** 3757–63
[28] Pellicer-Porres J, Segura A, Ferrer-Roca Ch, Martínez-García D, Sans J A, Martínez E, Itié J P, Polian A, Baudelet F, Muñoz A, Rodríguez-Hernández P and Munsch P 2004 High pressure structural study of the $CuGaO_2$ delafossite *Phys. Rev.* B **69** 024109
[29] Pellicer-Porres J, Segura A, Gilliland A S, Muñoz A, Rodríguez-Hernández P, Kim D, Lee M S and Kim T Y 2006 On the band gap of $CuAlO_2$ delafossite *Appl. Phys. Lett.* **88** 181904